

Determination of the rheological properties of aqueous solutions of branched PEO-PPO-PEO copolymers. Confrontation with small-angle neutron scattering studies.

Christelle PERREUR⁽¹⁾, Jean-Pierre HABAS⁽¹⁾, Jean PEYRELASSE^{(1)*}, Alain LAPP⁽²⁾, Jeanne FRANCOIS⁽¹⁾

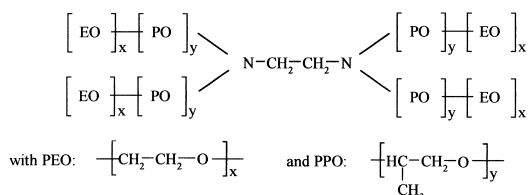
(1) : Laboratoire de physicochimie des polymères UMR 5067, Université de Pau et des Pays de l'Adour, Avenue de l'Université, 64000 PAU (FRANCE)

(2) : Laboratoire Léon Brillouin, CEA Saclay, 91191 GIF-sur-YVETTE (FRANCE)

SUMMARY: The physico-chemical properties of Tetronic[®] 908 in aqueous solution have been explored on a wide range of temperature and concentration. This system presents interesting rheological properties depending on the polymer concentration in solution, and temperature. For weight percentage p comprised between 5% and 20%, the viscosity of the solution passes through a maximum. Small angle neutron scattering experiments show that the increase in the viscosity is due to the progressive aggregation of the chains. For higher weight percentages, the viscosity of the system diverges and the mixture becomes "gel-like". SANS studies of the same solution indicate that the micelles are organized in a cubic structure. We have developed a model which suitably describes the SANS curves of the system in the region where micelles are formed. It allows the calculation of several parameters (volume fraction of the micelles, size, composition). The evolution of these parameters with temperature and polymer concentration is detailed. Comparisons with models of literature are discussed.

Introduction

Many reports have been published over the last decade on the aqueous solution properties of blocks copolymers (PEO)-(PPO)-(PEO). These compounds are non-ionic surfactants and have a wide variety of applications in fields ranging from medicine to petroleum industry. At low temperatures, both PEO and PPO blocks are water soluble; however, when the temperature is increased, PPO becomes insoluble. This amphiphilic character gives rise to a wide range of structures, depending on various parameters such as the length of the PEO and PPO sequences, temperature and polymer concentration. At low temperatures and concentrations, the copolymers exists in solution as individual molecules *ie* unimers. When the temperature is increased, these unimers self-associate to form micelles. If the concentration is high enough, a



Our work aims to correlate viscosimetric and rheological results with structural information derived from small-angle neutron scattering experiments. In particular, our study deals with the transition zone above the critical micellization temperature (CMT) where an equilibrium between unimers and micelles should exist. Indeed, if many authors have determined the temperature domain associated with unimers \leftrightarrow micelles transition, the equilibrium state has never been fully characterized^{4, 8, 12-14}).

Samples: In this paper, we have studied the properties of T908 for which the number of EO and PO units per branch are respectively $x = 114$ and $y = 21$ ($M = 25000 \text{ g mol}^{-1}$). Aqueous solutions were prepared at low temperature under stirring, using twice-distilled water for all rheological experiments and deuterated water, D_2O , for SANS studies. For this study, the weight percentage p of polymer is comprised between 1% (w/w) and 50% (w/w) and the

temperature range from 5°C to 80°C.

Experimental methods: Viscosimetric measurements were performed using Ubbelohde capillary tubes. The dynamic rheological properties were studied using a Rheometric Scientific DSR[®]. This apparatus is a stress-controlled rheometer with a Couette geometry working within the angular frequency range from 10^{-4} rad s⁻¹ to 10^2 rad s⁻¹. SANS experiments were performed at the Laboratoire Léon Brillouin, CE de Saclay (France) on the PAXY spectrometer (wavelength of 8 Å).

Results and discussion

Rheological studies : Viscosimetric studies of aqueous solutions of T908 showed that the general behavior of the system was strongly dependent on the weight percentage value (p) of polymer in the solution. For p ranging between 10 and 20%, the viscosity of the solution passed through a maximum (figure 1).

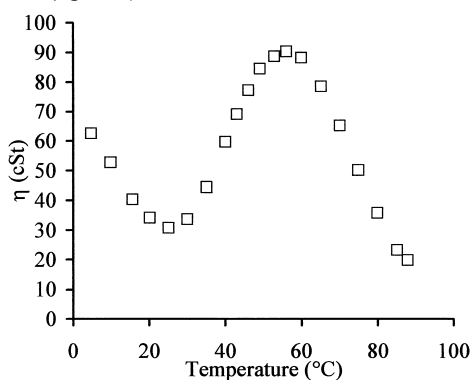


Fig. 1 : Evolution of the kinematic viscosity of a 20% solution according to temperature.

For p higher than 20%, we did not observe any maxima on the curves $\eta = f(T)$. But, above a well defined temperature labeled T_c , depending on concentration, the viscosity of the solution increased abruptly (figure 2). Above T_c , the mixture was unable to flow and, at first sight, it became “gel-like”.

Taking into account the published literature for similar polymeric solutions ⁷⁾, we can assume that, at low temperatures, the sample is a solution of unimers. At temperatures higher than the

critical value T_1 , the hydrophobicity of PPO is sufficient such that micelles form. The increase of the volume fraction of micelles subsequently induces a rise in viscosity (for $p > 2\%$).

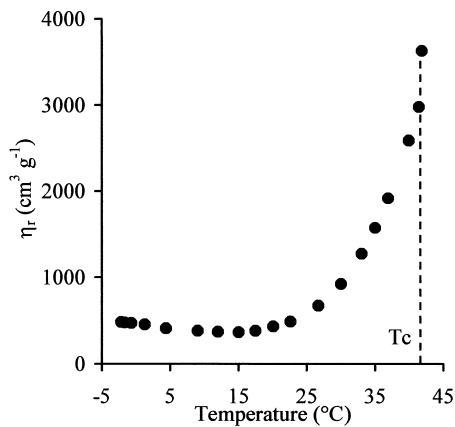


Fig. 2 : Temperature dependence of the viscosimetric behavior of a 30% solution.

SANS studies of the solutions should provide detailed informations to interpret the evolution of the viscosity. Determination of the critical temperatures, T_1 and T_c , allows a phase diagram to be drawn (figure 3).

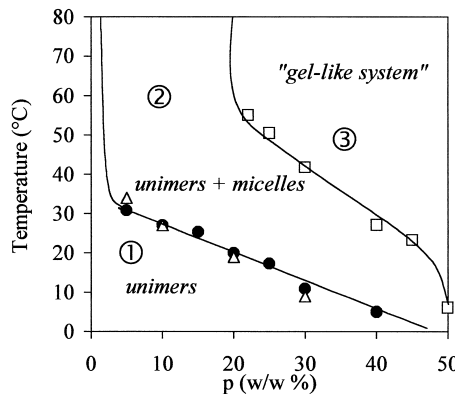


Fig. 3 : Phase diagram of aqueous solutions of Tetronic 908. Miscellisation temperature determined by viscosimetry (●), by SANS (Δ). Transition temperature to “gel-like system” (□)

Spectromechanical analyses of a 30% solution of Tetronic 908 permitted a study of the evolution of the rheological properties of the system with temperature (figure 4). Below 40°C and in the frequency domain, the flow zone of the polymeric solution is described. For

temperatures higher than 41°C, the presence of a crossover means that the solution behaves as an entangled polymer. Thus, the structure of the solution in the zone 3 of the phase diagram, is not a gel, this is contrary to assessments of various authors ^{2, 5, 11}).

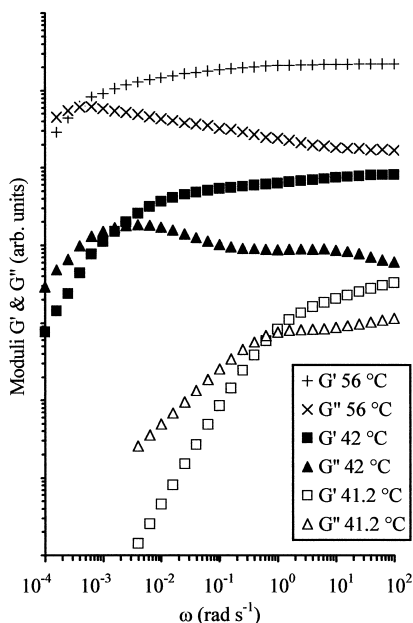


Fig. 4 : Spectromechanical analyses of a 30 % solution. The effect of temperature.

SANS studies : For dilute solutions ($p=1\%$) and in the zone 1 of the phase diagram, the curve of the scattered intensity $I(q)$, seemed to vary as a Debye function but the concentration was still too high to allow the calculation of the radius of gyration and molar weight of unimers. In the same zone of the phase diagram but for concentrated solutions, the unmicellized system behave as homogenous mixtures. For systems in the zone 2 or 3 of the phase diagram, the curve $I(q)$ presented a maximum whose intensity grew with temperature (figure 5).

In the zone 3 of the phase diagram, some small peaks of higher order, appeared on the curve of the scattered intensity. It indicated the transition to an organized phase inducing a high viscosity system. If we name q_1, q_2, q_3 the respective values of q at the successive maxima of the intensity, the ratios $\frac{q_2}{q_1}$ and $\frac{q_3}{q_1}$ were equal to $\sqrt{2}$ and $\sqrt{3}$. This revealed the presence of a local cubic structure.

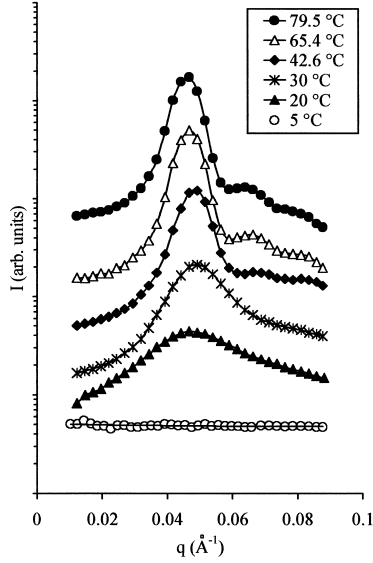


Fig.5 : Effect of temperature on the scattered intensity of a 30% solution

When intermicellar correlations become significant, and for a monodisperse system of particles, the scattered intensity $I(q)$ can be written as the product of the particle form factor $P(q)$ and the structure factor $S(q)$:

$$I(q) = N \times \Delta\rho^2 \times P(q) \times S(q)$$

where N is the number density of scatterers and $\Delta\rho^2$, the contrast factor.

$$S(q) \text{ is calculated with } S(q) = \frac{1}{1 + 24\Phi_{hs}G(x, \Phi_{hs})/x}$$

where $x = 2qR_{hs}$, R_{hs} is the hard sphere interaction radius, Φ_{hs} is the hard sphere volume fraction.

$$G(x, \Phi_{hs}) = A(x) + B(x) + C(x)$$

$$A(x) = \frac{\alpha}{x^2} [\sin(x) - x \cos(x)]$$

$$B(x) = \frac{\beta}{x^3} [2x \sin(x) + (2 - x^2) \cos(x) - 2]$$

$$C(x) = \frac{\gamma}{x^5} [-x^4 \cos(x) + 4(3x^2 - 6) \cos(x) + 4(x^3 - 6x) \sin(x) + 24]$$

The parameters α , β and γ are defined by:

$$\alpha = \frac{(1 + 2\Phi_{hs})^2}{(1 - \Phi_{hs})^4} \quad \beta = \frac{-6\Phi_{hs}(1 + \Phi_{hs}/2)^2}{(1 - \Phi_{hs})^4} \quad \gamma = \frac{\Phi_{hs}(1 + 2\Phi_{hs})^2}{2(1 - \Phi_{hs})^4}.$$

The form factor $P(q)$ is that of a hard sphere and is given by the equation :

$$P(q) = \left[\frac{4\pi}{3} R_c^3 \times \frac{3j_1(qR_c)}{qR_c} \right]^2 \quad \text{with } j_1 \text{ is the first order spherical Bessel function defined by}$$

$$j_1(x) = \frac{\sin(x) - x \cos(x)}{x^2}.$$

Litterature provides different models. The simplest one is that of Mortensen who assumes a monodisperse suspension of dense spheres with a sharp interface⁷⁾. This author has postulated that the core of radius R_c , holds the totality of PPO units and a small percentage of PEO. The major part of PEO forms a hydrated corona but is neglected in the calculations. Goldmints use a two shells model where the micelle is assimilated to a core of radius R_c surrounded by a corona of radius R_m ⁹⁾. Liu's model (adhesive hard spheres) is more complex since it takes into account the possible attractive interactions between micelles⁸⁾.

All these authors set different hypotheses: i) the radius R_m of the micelle is assumed identical to the radius of the hard sphere $R_m = R_{hs}$; ii) the scattering length densities (SLD) of PO and EO are equal; iii) water is present both in the core and the corona of the micelle. We have tried to fit the neutron scattering curves with the different models previously outlined. Mortensen's and Goldmints's models correctly describe the position and the amplitude of the peak, but they considerably deviate from experimental data at low and high values of q . Liu's model overestimates the principal peak of intensity (figure 6).

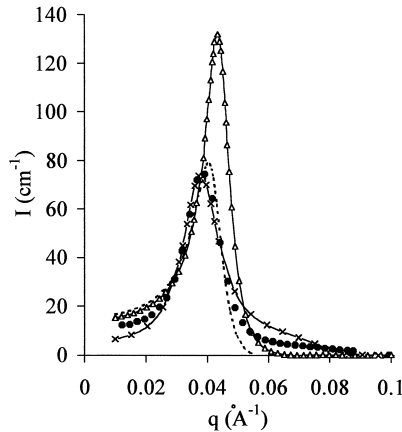


Figure 6 : Comparison of different models of the literature to a 20% solution at $T = 83^\circ\text{C}$. Experience (●); Liu (Δ); Goldmints (---); Mortensen ($- \times -$).

In order to better explain our experimental results, we propose a quite different model. It is a three shells model with four adjustable parameters. For this multilayer model, we can write:

$$P(q)\Delta\rho^2 = \sum_1^3 \left(\frac{4}{3} R_i^3 (\rho_i - \rho_{i+1}) \frac{3j_1(qR_i)}{qR_i} \right)^2$$

where j_1 is the first order spherical Bessel function previously defined, R_i is the radius of the i^{th} layer, and ρ_i its scattered length density (SLD). For $i = 3$, ρ_4 is the SLD of the solvent.

The hypotheses of our model are that i) all micelles are identical, ii) the core of radius R_1 contains the totality of PPO in close packing conditions, iii) the first layer of thickness $R_2 - R_1$ is constituted by a fraction χ of PEO units in the micelles, iv) the corona of external radius $R_m = R_{hs}$ is an homogenous mixture of water and residual PEO units. To calculate the structure factor $S(q)$, we have used the equations previously described.

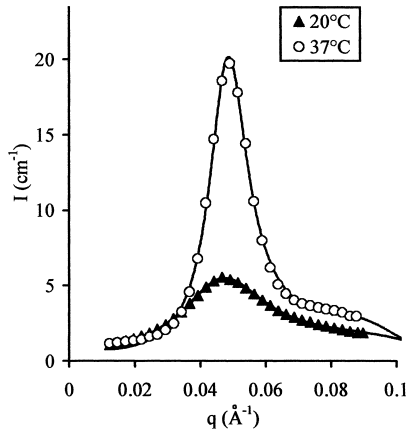


Figure 7 : Description of SANS curves with our model. Example of application to a 30% solution. Symbols : data ; line : fitting

The four adjustable parameters are the volume fraction Φ and the radius R_m of micelles, the fraction χ of PEO in the dense layer and the concentration C_m of micellized polymer (g cm^{-3}).

By numerical fitting, we have determined the best values of the four parameters for all studied solutions. It is worth noting that for all concentrations and at each temperature, the agreement between the model and the experimental data is very good (figure 7). We have used the same values of scattering length densities of EO, PO and D_2O as found in literature¹⁵⁻⁸). The different volume fractions of micelles Φ according to temperature for all solutions studied are plotted in figure 8. The extrapolation at $\Phi = 0$ gives the critical temperature of micellisation whose value is in good agreement with the results of the viscosimetric characterization. For p

$\leq 22\%$, Φ passes through a maximum value. This result explains the existence of the maximum of viscosity for these solutions. For $p \geq 30\%$ and at the transition temperature T_c , we can also note a discontinuity in the increase of the volume fraction. Then, Φ tends to a constant value.

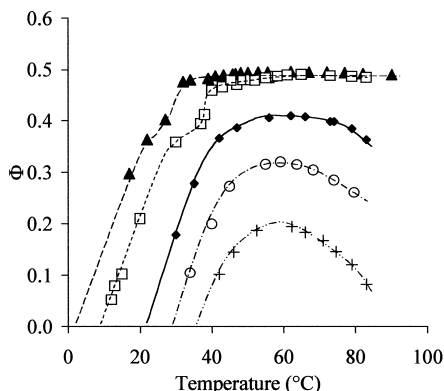


Figure 8 : Evolution of the volume fraction of the micelles versus T for different solutions: 5% (+), 10% (O), 20% (◆), 30% (□), 40% (▲)

The size of the micelles depended strongly on the initial concentration of polymer in solution. After a rapid increase above CMT, the size of the micelles tends to a limiting value at high temperature which increases when the weight percentage p is decreased. This last result shows that the size of the micelles not only depends on the aggregation number (figure 9).

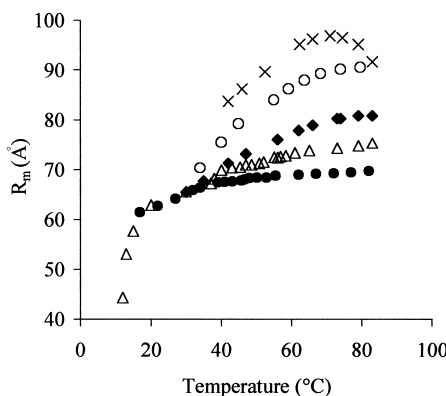


Figure 9 : Effect of temperature on the micelles radius for different solutions 5% (×), 10% (O), 20% (◆), 30% (Δ), 40% (●)

It is now possible to determine the aggregation number $N_{agg} = \frac{4\pi C_m N_a R_m^3}{3\Phi M}$, where M is the molar weight of the polymer and N_a the Avogadro number (fig. 10 for p = 10%). For low values of the aggregation, the curve $N_{agg} = Cte$ is parallel to the limit between the zones 1 and 2, ($N_{agg} = 1$). Then, the formation of micelles with $N_{agg} < 15$, eases when the concentration increases.

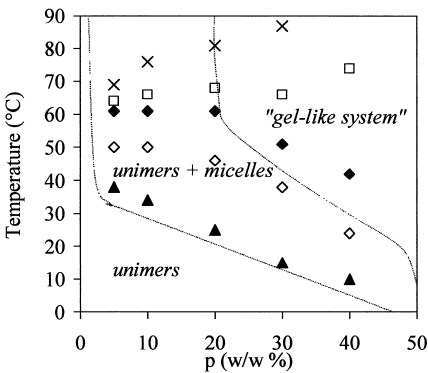


Figure 10 : Examples of curves $N_{agg} = Cte$ plotted on the phase diagram.
6 (▲), 10 (◊), 13 (◆), 15 (◻), 18 (×)

A reverse phenomenon is observed when N_{agg} is at a high value. This could be due to the high viscosity of the medium as the migration of unimers to micelles would require more thermal energy.

Conclusion

The model proposed here, shows that T908 produces micelles that can be considered as spherical units with three shells above critical conditions of temperature and concentration. This model satisfactorily describes the experimental curves of the scattered intensity in SANS experiments with a limited number of parameters. Many structural informations can be easily derived and plotted according to temperature or concentration of the polymer. Precise correlations between the structure of the material and its rheological properties are possible. Our model can be easily applied to different materials which form similar micellar structures.

References

[1] – G. Wanga, H. Hoffmann, and W. Ulbricht, *Colloid polym. Sci.* **268**, 101 (1990).
[2] – P. Bahadur and K. Pandya, *Langmuir* **8**, 2666 (1992).
[3] – S. Hvidt, *Colloids and Surfaces* **112**, 201 (1995).

- [4] – O. Glatter, G. Scherf, K. Schillen and W. Brown, *Macromolecules*, **27**, 6046 (1994).
- [5] – B. Jeong, D.S. Lee, J. Shon, Y.H. Bae and S.W. Kim, *J. polym. Sci.* **37**, 751 (1999).
- [6] – S.M. King, R.K. Heenan, V.M. Cloke and C. Washington, *Macromolecules*, **30**, 6215 (1997).
- [7] – K. Mortensen, *J. Phys.: Condens. Matter*, **8**, A103 (1996).
- [8] – Y.C. Liu, S.H. Chen and J.S. Huang, *Phys. Rev E*, **54**, 1696 (1996).
- [9] – L. Goldminst, G.Y. Yu, C. Booth, K.A. Smith, *Langmuir*, **15**, 1651 (1999).
- [10] – C. Wu, T. Liu, B. Chu, *Macromolecules*, **30**, 4574 (1997).
- [11] – R.K. Prud'homme, G. Wu and D.K. Schneider, *Langmuir*, **12**, 4651 (1996).
- [12] – Z. Zhou and B. Chu, *Macromolecules*, **27**, 2025 (1994).
- [13] – J.R. Lopes and W. Loh, *Langmuir*, **14**, 750 (1998).
- [14] – P. Alexandridis, J. F. Holzwarth and T.A. Hatton, *Macromolecules*, **27**, 2414 (1994).
- [15] – P. Linse, *Macromolecules*, **27**, 6404 (1994).
- [16] – W. Hoover and F.H. Ree, *J. Chem. Phys.*, **49**, 3609 (1968)

